

https://doi.org/10.1070/QEL17571

Suppression of nonlinear distortion in a high-speed multichannel communication line with variable quadratic dispersion compensation

E.G. Shapiro, D.A. Shapiro

Abstract. **We report a numerical simulation of the propagation of short (25 ps) 8QAM pulses for two polarisations in a nine-channel communication line with a frequency band of 80 GHz. It is shown that the use of large-chirp pulses and different dispersion compensators leads to effective suppression of nonlinear distortions and significantly improves the signal quality in a multichannel communication line due to the rapid pulse broadening.**

Keywords: *fibre-optic communication lines, mathematical modelling, nonlinear Schrödinger equation, wavelength division multiplexing, chirp.*

1. Introduction

The permanent need for increasing the traffic throughput in fibre lines by about 40% per year stimulated the development of new optical communication technologies [1, 2]. They include wavelength division multiplexing (WDM) of channels [3], coherent detection [4], and electronic compensation for accumulated dispersion [5]. Wavelength division multiplexing allows parallel data transmission at different wavelengths, thereby increasing the channel capacity by two orders of magnitude. Coherent detection is a method for measuring the complex amplitude, which makes it possible to organise phase and amplitude keying together with polarisation multiplexing and transmit several bits in one pulse using special spectrally efficient modulation formats [6].

During transmission, the signal is distorted mainly due to amplifier noise and Kerr nonlinearity. Kerr nonlinearity gives rise to a number of effects, such as interchannel coupling, a change in the pulse shape due to adjacent bits in one channel (pattern effect), interaction of a signal with amplified noise, etc. Each nonlinear effect increases the probability of erroneous signal recognition. For example, intra-channel cross-modulation causes jitter and even the appearance of ghost pulses observed in the experiment [7]. An important task is to develop methods for suppressing nonlinearity due to dispersive spreading of pulses. Chromatic and polarisation dispersion can be compensated for at the receiving end of the line using coherent reception and digital processing without intermediate compensators, and nonlinear effects are noticeably reduced due to the small amplitude of pulses after spreading [8, 9].

At the same time, dispersive spreading occurs rather slowly, and so it was proposed to impart a large chirp to the pulses at the transmitter, and to compensate for it at the receiver during single-channel transmission [10]. Then, when the signal propagates, its amplitude will be small, and therefore, nonlinear noise will decrease. The authors of Ref. [11] proposed to use, in addition to the chirp, variable dispersion compensation, i.e., different compensators in different sections of the line. It was shown that nonlinear distortion in one channel is reduced. At the same time, a pulse with a large chirp has a wide spectrum, and its energy can go into neighbouring channels. Therefore, the problem of chirped pulses in a WDM communication line was not solved.

In this paper, we consider the propagation of optical pulses in nine channels with a frequency band of 80 GHz each. We numerically simulated the propagation of Gaussian pulses with a bit interval of 25 ps in the framework of coupled nonlinear Schrödinger equations [12–14] for two polarisations. In addition, to reduce the Kerr nonlinearity in the calculations, variable dispersion compensators were used, providing a quadratic increase in the compensation in the line from section to section. As a result, almost all of the accumulated dispersion was compensated for at the end of the line. It is shown that the use of a large chirp simultaneously with variable dispersion compensation significantly improves the signal quality in a multichannel system.

The paper also shows that the peak power of Gaussian pulses passed through an optical filter decreases the faster the larger the chirp value. By a peak pulse power, we mean the maximum power value. Thus, the peak power is reached in the middle of the bit slots for each individual Gaussian pulse train. Peak power causes phase distortion, and so its steep decrease reduces nonlinear noise.

2. Peak power

After passing through a rectangular filter with width L and subsequent chirping, a Gaussian pulse $a(t) = \exp[-t^2/(2T_0^2)]$, where T_0 is the pulse width parameter, is given by the formula

$$a(t) = \exp\left(\frac{\mathrm{i}C}{2T_0^2}t^2\right)\frac{T_0}{\sqrt{2\pi}}\int_{-L/2}^{L/2}\exp\left(-\frac{1}{2}T_0^2k^2 + \mathrm{i}kt\right)\mathrm{d}k$$

$$= \frac{1}{2}\exp\left(-\frac{1-\mathrm{i}C}{2T_0^2}t^2\right)\left\{\mathrm{erf}\left[\frac{T_0}{\sqrt{2}}\left(\frac{L}{2} - \mathrm{i}\frac{t}{T_0^2}\right)\right] + \mathrm{c.c.}\right\}.$$

Filtering changes the pulse shape, especially for small values of the width parameter T_0.

E.G. Shapiro, D.A. Shapiro Institute of Automation and Electrometry, Siberian Branch, Russian Academy of Sciences, prosp. Akad. Koptyuga 1, 630090 Novosibirsk, Russia; e-mail: shapiro@iae.nsk.su

Received 20 April 2021; revision received 9 May 2021
Kvantovaya Elektronika **51** (7) 635–638 (2021)
Translated by V.L. Derbov

First, we obtain an approximation for the error function using the Taylor series expansion and the formula

$$\frac{d^{n+1}\mathrm{erf}(x)}{dx^{n+1}} = (-1)^n \frac{2}{\sqrt{\pi}} H_n(x)\exp(-x^2),$$

where $H_n(x)$ is a Hermite polynomial [15]. We set $x = T_0 L \times (2\sqrt{2})^{-1}$ and the increment $\Delta x = -it/(\sqrt{2}\,T_0)$, then in the vicinity of $t = 0$, the expansion of $a(t)$ to the fourth order of smallness takes the form

$$a(t) \approx = \frac{1}{2}\exp\left(-\frac{1-iC}{2T_0^2}t^2\right)\left\{\mathrm{erf}\left(\frac{T_0 L}{2\sqrt{2}}\right) + \frac{\exp(-T_0^2 L^2/8)L}{2\sqrt{2\pi}\,T_0}\right.$$

$$\left.\times\left[t^2 - \frac{1}{12}\left(\frac{T_0^2 L^2}{4} - 3\right)\frac{t^4}{T_0^2}\right]\right\}. \qquad (1)$$

The pulse shape $A(z,t)$ with the boundary condition $A(0,t) = a(t)$ during propagation along the fibre is determined by the equation

$$i\frac{\partial A}{\partial z} = \frac{\beta_2}{2}\frac{\partial^2 A}{\partial t^2}, \qquad (2)$$

where β_2 is the parameter of the dispersion effect; t is the time; and z is the distance (the nonlinearity is ignored).

We denote $\tilde{D} = -\beta_2/2$. Then the solution of Eqn (2) is written as

$$A(z,t) = \int_{-\infty}^{\infty} A_k(z)\exp(ikt)\frac{dk}{2\pi}, \quad A_k(z) = A_k(0)\exp(-i\tilde{D}k^2 z),$$

$$A_k(0) = \int_{-\infty}^{\infty} A(0,t)\exp(-ikt)\,dt.$$

With the broadening of the optical pulse, the peak power at $t = 0$ decreases. With expansion (1) taken into account, the dynamics of the peak pulse power in a linear medium is given by the formula

$$A(0,z) = \mathrm{erf}\left(\frac{T_0 L}{2\sqrt{2}}\right)\frac{1}{\lambda} + \frac{\exp(-T_0^2 L^2/8)\,T_0 L}{2\sqrt{2\pi}(1-iC)}\left(\frac{1}{\lambda} - \frac{1}{\lambda^3}\right)$$

$$-\frac{\exp(-T_0^2 L^2/8)\,T_0 L}{8\sqrt{2\pi}(1-iC)^2}\left(\frac{T_0^2 L^2}{4} - 3\right)\left(\frac{1}{\lambda} - \frac{2}{\lambda^3} + \frac{1}{\lambda^5}\right), \qquad (3)$$

$$\lambda = \sqrt{1 + \frac{2i(1-iC)\tilde{D}z}{T_0^2}}.$$

Phase distortions of the signal are due to the Kerr nonlinearity, and they are the greater, the greater the peak power of the pulses. For the propagation of an ideal Gaussian pulse $F(t,0) = \exp[-(1-iC)t^2/(2T_0^2)]$, $L \to \infty$, in a linear medium, the derivative $\partial|F(0,z)|^2/\partial z \sim -C$, i.e., the peak power decreases with increasing z, the faster the larger the chirp C. The use of filters that separate the channels changes the shape of the pulses. The smaller the parameter T_0, the more noticeable these changes. The decrease in the peak power of the pulse at a finite value of L also occurs the faster, the larger the parameter C. This can be shown by direct differentiation of $|A(0,z)|^2$ using expansion (3).

Figure 1 shows the dependences of $|A(0,z)|^2$ on the distance z according to Eqn (3) for $C = 0$, 1, 10, and 20 at $L =$ 80 GHz. It is seen that the peak power sharply decreases at large values of C. Therefore, for pulses with a large chirp, instead of the nonlinear Schrödinger equation, one can use the approximate equation (2). For comparison, the dots indicate the same dependences calculated within the framework of the nonlinear Schrödinger equation with zero damping. With an increase in chirp, the deviation practically disappears and the curves are in good agreement with the numerical calculation. The peak power decreases monotonically with increasing distance.

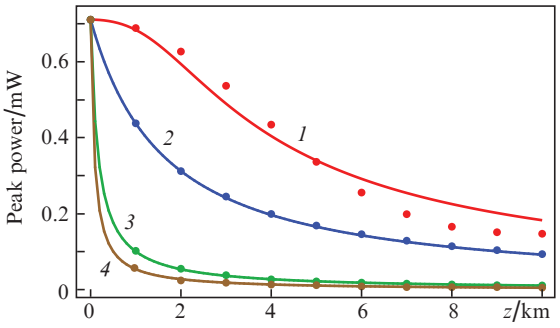

Figure 1. Peak power $|A(0,z)|^2$ vs. distance z for $C = (1)$ 0, (2) 1, (3) 10, and (4) 20 (the points correspond to the numerical calculation taking the Kerr nonlinearity into account). The curves are plotted according to the approximate formula (3).

As a large-chirp Gaussian pulse train propagates, adjacent bits begin to overlap and each individual bit is propagated in multiple bit slots. Broadened pulses are less prone to nonlinear distortion. The propagation regime without high peak powers begins the faster, the larger the parameter C. Thus, the use of a large chirp causes a sharp decrease in the peak power of the pulses and thereby suppresses the distortions caused by nonlinearity. Below are the results of numerical simulation of the propagation of an 8QAM signal in nine channels of a communication line with a length of 1500 km only for polarisation A_x, since the results for A_x and A_y are the same. The plots refer to the central channel.

3. Numerical simulation

The communication line consisted of 15 periodic sections of the form

SMF (100 km) + EDFA + DC(i),

where SMF is a standard single-mode fibre; EDFA is an erbium-doped fibre amplifier; and DC(i) is a dispersion compensator with number i. Let us denote by d_i the dispersion compensated by the DC(i) device. The parameters of the SMF fibre used in the calculations are shown below.

Attenuation at $\lambda = 1550$ nm/dB km^{-1}	0.2
Effective area/μm^2	.80
Chromatic dispersion/ps nm^{-1} km^{-1}	.17
Dispersion slope/ps nm^{-2} km^{-1}	.0.07
Nonlinear refractive index/m^2 W^{-1}	2.7×10^{-20}

In this paper, we used variable dispersion compensation, i.e., devices with different compensation values. This method of removing dispersion distortions was proposed in Ref. [11], where a simulation of the propagation of pulses in a communication line was performed with devices, whose compensation values form an arithmetic progression, and the average line dispersion is equal to zero. Variable dispersion compensation reduces nonlinear distortion because optical pulses recover shape only at the end of the communication line.

The accumulated dispersion from 15 sections of the SMF fibre was 25500 ps nm^{-1}. In our case, the values of dispersion compensation d_i grow quadratically and the total corresponding compensation is equal to 25500 ps nm^{-1}. We placed the first compensator after the 5th section, i.e. $d_{1-4} = 0$. For other d_i, the following values were taken: d_5 = 628 ps nm^{-1}, d_6 = 904.4 ps nm^{-1}, d_7 = 1231 ps nm^{-1}, d_8 = 1608 ps nm^{-1}, d_9 = 2035 ps nm^{-1}, d_{10} = 2512 ps nm^{-1}, d_{11} = 3040 ps nm^{-1}, d_{12} = 3617 ps nm^{-1}, d_{13} = 4246 ps nm^{-1}, d_{14} = 4924 ps nm^{-1}, and d_{15} = 754 ps nm^{-1}.

It was assumed that periodic compensation of dispersion is implemented using modern devices with low signal attenuation based on Bragg gratings [16, 17]. A white Gaussian noise model was taken to describe the amplified spontaneous emission (ASE) noise of point erbium amplifiers. We ignored the distortions caused by polarisation mode dispersion.

The signal was transmitted in nine channels with a spectral separation of 80 GHz. Before channelisation, the optical pulses were passed through an 80 GHz rectangular filter to avoid distortions from the code sequences of adjacent channels. After combining the channels, the signal was chirped before entering the line, which mathematically means multiplying the bit interval with number n by $\exp[\mathrm{i}C(t - nT)^2 \times (2T_0^2)^{-1}]$.

We have considered the transmission of information, which is encoded by eight phase-amplitude levels of Gaussian pulses for the polarisations A_x and A_y. Figure 2 shows the modulation scheme for the 8QAM format in the plane of the complex amplitude of a single polarisation signal.

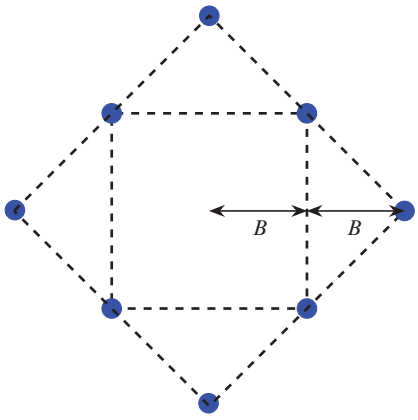

Figure 2. Schematic representation of the 8QAM format in the complex amplitude plane. The dots indicate the amplitude values (A_x or A_y) for different bit sequences.

Gaussian pulses before the filter were specified by the formulae

$$A_x(t) = \sum_n a_{x_n}(t - nT), \quad A_y(t) = \sum_n a_{y_n}(t - nT),$$

$$a_{x_n}(\tau) = X_n \xi_{x_n} \exp\left(-\frac{\tau^2}{2T_0^2}\right), \quad a_{y_n}(\tau)\, Y_n \xi_{y_n} \exp\left(-\frac{\tau^2}{2T_0^2}\right),$$

where the independent quantities X_n, Y_n are equal to either B or $2B$ with probability 1/2. If $X_n = B$, then ξ_{x_n} is a random variable taking with probability 1/4 one of the values from the set $\{e^{i\pi/4}, e^{-i\pi/4}, e^{3i\pi/4}, e^{-3i\pi/4}\}$; if $X_n = 2B$, then ξ_{x_n} takes one of the values from the set {1, i, 1, –i} also with probability 1/4. The quantity ξ_{y_n} is defined similarly. The bit interval is T = 25 ps, the pulse width parameter is T_0 = 6 ps.

Figure 3 shows the power spectra of the input signal and the signal after chirping with the parameter C = 10. It can be seen that the chirp broadens the signal frequency band; therefore, to separate the channels at the receiving device, the bit interval with number n was multiplied by $\exp[-\mathrm{i}C(t - nT)^2 \times (2T_0^2)^{-1}]$. Then, using filters, individual channels were selected.

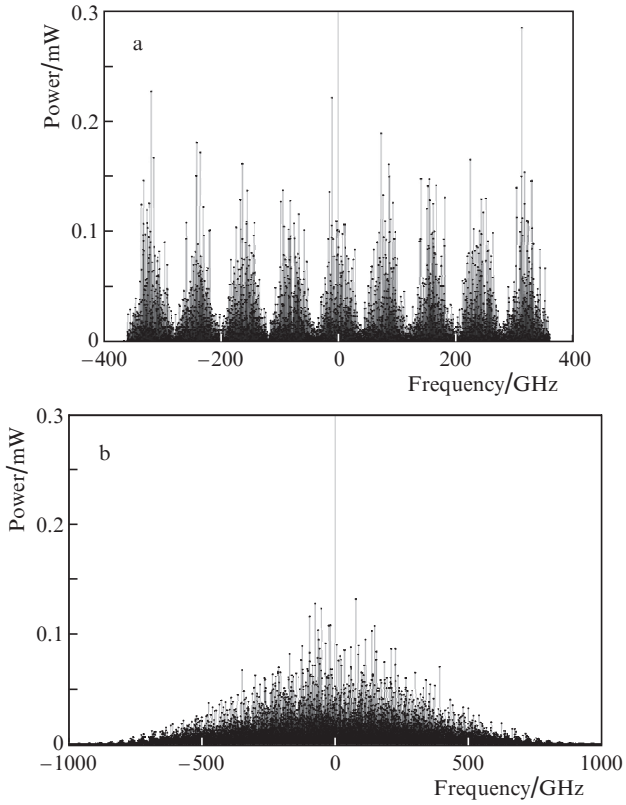

Figure 3. Power spectrum of (a) input and (b) output signals (C = 10).

To demonstrate the suppression of nonlinear noise using a large chirp, we simulated signal propagation in a line with ideal EDFAs, i.e., in the absence of noise. Figure 4 shows the signal diagrams of the central channel for the chirp parameters C = 0 and 20; the peak power is 0.94 mW. The probability of errors without a chirp was 3.7×10^{-4}. In the case of using the chirp, there were no errors in the sample of 18000 bits.

One of the main causes of signal distortion is amplifier noise. Figure 5 shows signal diagrams taking into account the noise of the amplifiers for the same values of parameter C. The error probabilities in Figs 5a and 5b are 1.54×10^{-3} and 2.5×10^{-4}, respectively. Thus, even if the signal is distorted by ASE noises, the error probability decreases markedly for a signal with a large chirp.

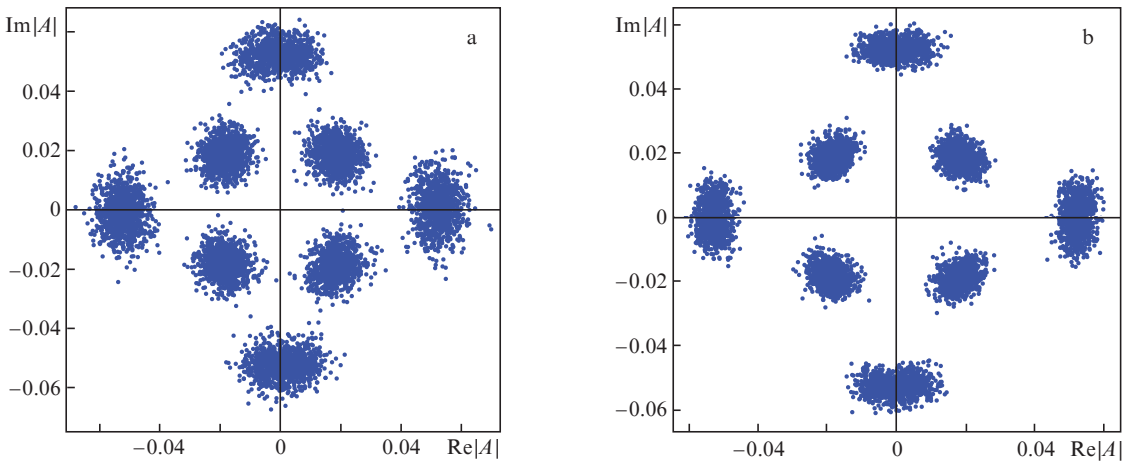

Figure 4. Signal diagrams of the bit sequence of the central channel for the chirp parameters C = (a) 0 and (b) 20; the peak power is $B^2 = 0.94$ mW.

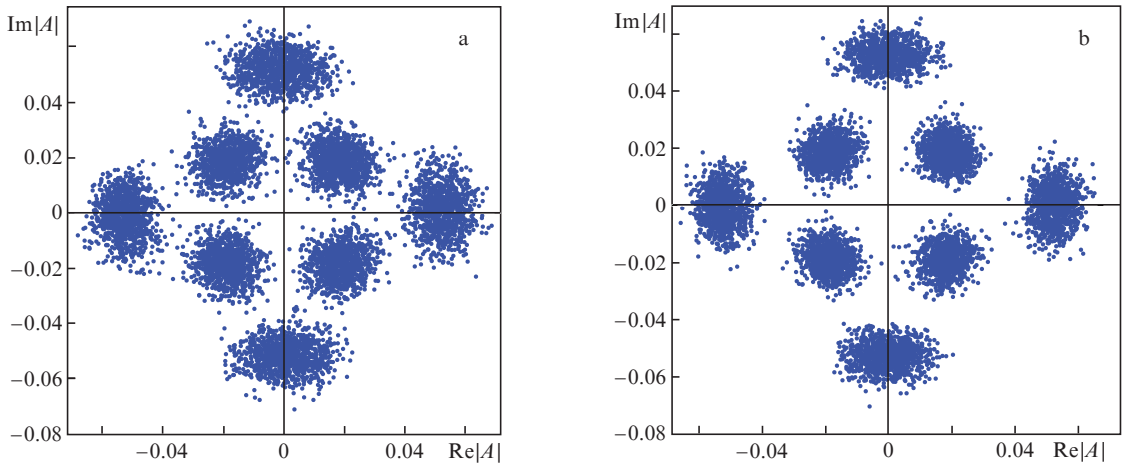

Figure 5. Signal diagrams taking into account the ASE noise of the amplifiers for C = (a) 0 and (b) 20; the peak power is $B^2 = 0.94$ mW.

4. Conclusions

We simulated the propagation of optical 8QAM pulses in a 9-channel communication line with quadratic dispersion compensation. It is shown that, despite the broadening of the frequency band, the chirp provides a higher signal quality. The advantage of a large chirp is substantiated analytically. Pulses with a large chirp are shown to quickly lose their peak power, which provides an effective reduction in nonlinear distortions. The results obtained can be useful both when choosing a design for a high-speed communication line, and when renovating existing lines.

Acknowledgements. The work was supported by the Ministry of Science and Higher Education of the Russian Federation (Project AAAA-A21-121012190005-2).

References

1. Richardson D.J. *Science*, **330**, 327 (2010).
2. Dianov E.M. *Foton-ekspress*, No. 1 (129), 18 (2016).
3. Yoo S.J.B. *J. Lightwave Technol.*, **14**, 955 (1996).
4. Ip E. et al. *Opt. Express*, **16**, 753 (2008).
5. Bülow H. et al. *J. Lightwave Technol.*, **26**, 158 (2008).
6. Winzer P.J. et al. *J. Lightwave Technol.*, **28**, 547 (2010).
7. Mamyshev P.V., Mamysheva N.A. *Opt. Lett.*, **24**, 1454 (1999).
8. Savory S.J. *Electron. Lett.*, **42**, 407 (2006).
9. Konyshev V.A. et al. *Quantum Electron.*, **46**, 1121 (2016) [*Kvantovaya Elektron.*, **46**, 1121 (2016)].
10. Shapiro E.G., Shapiro D.A. *Quantum Electron.*, **50**, 184 (2020) [*Kvantovaya Elektron.*, **50**, 184 (2020)].
11. Shapiro E.G., Shapiro D.A. *Opt. Commun.* (2020); https://doi.org/10.1515/joc-2020-0097.
12. Yushko O.V. et al. *Quantum Electron.*, **45** (1), 75 (2015) [*Kvantovaya Elektron.*, **45** (1), 75 (2015)].
13. Agrawal G.P. *Applications of Nonlinear Fiber Optics* (San Diego: Academic Press, 2001; St. Petersburg: Lan', 2011).
14. Poggiolini P. et al. *J. Lightwave Technol.*, **32**, 694 (2013).
15. Olver F.W.J. et al. *NIST Handbook of Mathematical Functions* (New York: Cambridge University Press, 2010).
16. Sumetsky M., Eggleton B. *J. Opt. Fiber Commun. Rep.*, **2**, 256 (2005).
17. Dar A.R., Jha R.K. *Opt. Quantum Electron.*, **49**, 108 (2017).